In Silico Studies on Fingolimod and Cladribine Binding to p53 Gene and Its Implication in Prediction of Their Carcinogenicity Potential

Karim Mahnam[1], Azadeh Hoghoughi[1]

1. Biology Department, Faculty of Science, Shahrekord University, Shahrekord, Iran

Abstract

Background: New drugs namely; cladribine and fingolimodare known to be effective in treatment of multiple sclerosis (MS). The interaction of these drugs with the promoter region of the p53 gene may alter p53role in cancer progression. The aim of this study was to known the interaction of these compounds with p53 gene.

Methods: Binding free energy of the cladribine, fingolimod and their modified drugs for the p53 gene promoter were investigated using docking, 100 ns molecular dynamics simulations and MM/PBSA calculation.

Results: The results showed that both cladribine and modified cladribine (replacing -OH on carbon 3′ ribose sugar with -CH3 group) can bind the minor groove of p53 promoter, and inhibit the binding of transcription factors and expression of p53. However, fingolimodand its derivatives showed relatively weaker interaction with p53 promoter

Conclusions: Based on in silico studies we showed that the binding of cladribine to the p53 gene is stronger than that of fingolimod, hence it seems that the former drug can pose potential carcinogenic effects. The binding power and carcinogenic effect of sm-fingolimod (removing four carbons from its aliphatic tail) is more than that of fm-fingolimod (removing one carbon from its aliphatic tail).

Keywords: Cladribine, Fingolimod, Molecular dynamics simulation, MM/PBSA, p53 gene

Introduction

Multiple sclerosis (MS) is a demyelinating inflammatory disorder of the central nervous system (CNS) with autoimmune responses. The degree of axonal destruction is variable (Calabresi, 2004). The route of MS is highly varied and unpredictable so that it may be initiated through reversible neurological deficits, followed by progressive neurological deteriorations (Navikas *et al.*, 1996).

The first oral disease-modifying drug approved food and drug administration (FDA) is Fingolimod (Gilenya, Novartis) (Fig. 1A) to postpone progression of physical disability in patients. Fingolimod is metabolized by sphingosine kinase to the active metabolite; fingolimod phosphate, which in turn blocks migration of lymphocytes from lymphnodes, thereby reducing the number of lymphocytes

*Corresponding author. Karim Mahnam, PhD.**
Biology Department, Faculty of Science, Shahrekord University,
P.O. Box: 8818634141,Shahrekord, Iran
Tel., +98-038-4424402; Fax, +98-38-4424419
Email: mahnam.karim@sci.sku.ac.ir

in peripheral blood (Cohen *et al.*, 2007). The possible mechanism of the therapeutic effect of fingolimod in MS is through the reduction of lymphocyte migration into the CNS (Francesca, 2007).
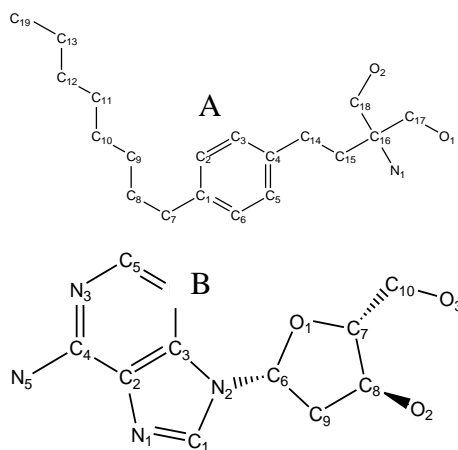

Figure 1. Structure of fingolimod (A) and cladribine (B).

Fingolimod has been associated with reduce heart rate (bradycardia) and usually fatal infections such as cancer (Cohen *et al.*, 2007). Another drug used to treat hairy cell leukemia (HCL, leukemic reticuloendotheliosis) and MS is cladribine (Leustatin, Litak and Movectro™) with chemical formula 2-chloro deoxyadenosine (CldAdo) (Fig. 1B). (http://www.medschat.com/search.asp?q=cladr ibine). It is a purine analog and acts as suppressor of the immune system. Possible side effects of the cladribine include fever, infection, anemia and cancer. CldAdo is taken up by cells, converted to 2-chloro-2′-deoxy adenosine triphosphate (CldATP), and

incorporated into DNA, thereby causes down-regulation of cellular ribonucleotidereductase and inhibit DNA synthesis (Foley *et al.*, 2004). TATA element of the promoter is recognized by TATA binding protein (TBP). Foley *et al* showed that positions in the TATA sequence are most severely affected by cladribine incorporation (Foley *et al.*, 2004).

In general, drug targets are cytoplasmic proteins, membrane receptors or membrane-bound proteins, nuclear proteins, DNA etc. Small aromatic compounds can bind DNA by two ways:

A: Covalent bond; through their functional groups irreversibly attached to DNA, leading to inhibition of DNA synthesis processes and cell death such as Cisplatin and Mitomycin (Elizondo-Riojas *et al.,* 2001).

B: Non-covalent bond; by intercalation (such as Triostatin, Actinomycin, Bleomycin) intominor groove binding such as; Netropsin, Distamycin and into major groove binding; such as Norfloxacin (Neidle *et al.*, 1987).

The tumor suppressor *p53* gene as an important tumor suppressor gene continually is transcribed to prevent cancer. *P53* gene is the most frequently mutated gene in human tumors (Vogelstein *et al.*, 2010). In some cancers, transcription of the p53 gene is reduced (Bai *et al.*, 2006).

The Molecular Mechanics/Poisson–Boltzmann Surface Area (MM-PBSA) method has been

used to calculate relative free energies of DAPI (4', 6-diamidino-2-phenylindole) into four sequences of DNA (Spacková *et al., 2003*). Currently the computational techniques are widely applied in chemistry and biology ranging from the quantum mechanics of molecules to the dynamics of large complex molecular aggregates. Molecular interactions steer chemical reactions, phase transitions and other physical phenomena and can be studied via molecular dynamics (MD) simulations, showing the detailed motion of molecules or atoms as a function of time. The MD simulations provide powerful links between the model equilibrium, minimal geometries of proteins and DNA and binding free energy of drugs (Karplus *et al.,* 2005). The calculation of relative binding free energies of ligands to a receptor has been used for better understanding of molecular interactions of proteins with small compounds and drugs design (Oostenbrink *et al.,* 2005).

In our ongoing project, we have performed some theoretical studies to investigate the mechanism of binding of cladribine and fingolimodto promoter of *p53* gene. In addition, the effect of some structural modifications of these drugs in binding their free energy to promoter of *p53* gene has been investigated. The expected results are implicated in knowing the mechanism underlying carcinogenicity of cladribine or fingolimod.

Methods

Promoter of *p53* gene has 52 pair nucleotides. The sequence of the 5´ to 3´ strand of promoter of *p53* gene that was applied for this study was 5´-GAGCCTCGCAGGGGTTGATGGGATTGG GGTTTTCCCCTCCCATGTGCTCAAG-3´ (Reisman *et al.,* 1993). 3D structure of *p53* promoter was generated via 3D-Dart (3DNA-Driven DNA Analysis and Rebuilding Tools) web server (haddock.science.uu.nl/ services/3DDART). Also, geometries of all ligands were obtained from Arguslab software (http://www.arguslab.com/arguslab.com/Argus Lab.html) via molecular mechanics methods under MM$^+$ force fields and used for docking and MD simulation studies. The atomic charges of all ligands were calculated with the Merz−Kollman electrostatic potential fitting procedure in the Gaussian quantum chemistry package (Frisch *et al.,* 1998). This was performed by means of a Hartee-Fock wave function obtained in a 6-31G* basis set for compatibility with the partial charges from the AMBER force field that was used for *p53* promoter (Amber99). The restrained electrostatic potential (RESP) charge calculation was done using this command: HF/6-31G* Pop=MK IOp (6/33=2, 6/41=10, 6/42=17) (Kim *et al.,* 2011). Cladribine was modified by replacing OH on carbon 3´ ribose

sugar with CH_3 group. Modification of fingolimod was done by removing one carbon (fm-fingolimod) or four carbons (sm-fingolimod) from the aliphatic hydrocarbon tails. All images were generated with Discovery Studio® Visualizer software (http://accelrys.com/products/discovery-studio). Theoretical studies were done in three following sections:

1. Docking

Autodock 4 software was used for docking studies (Morris *et al.*, 1998). The grid box size was set at 90×90×118 Å and spacing between grid points 0.375 angstrom. The *p53* promoter structures were fixed during docking, while the drugs were flexible. Grid searching was performed by a local search genetic algorithm (LGA) to locate the ligands in the lowest binding energy. Routine procedures and default parameters were used in the docking except dstep, tstep and qstep that were considered 0.5 Å, 0.5°, 5° respectively (Majumdar *et al.*, 2011).

All ligands (cladribine, modified cladribine, fingolimod, first and second modified fingolimod) were docked on *p53* promoter. Two hundred docking runs were performed for each docking. The best pose with the lowest binding energy and the most populated conformation in each cluster was chosen as the initial structure in the molecular dynamics simulation.

2. Molecular dynamic simulations

Five molecular dynamics simulation of ligands complexes with *p53* promoter sequence were performed. The cycle time for each simulation was 20 ns. Then, one hundred ns MD simulations were applied. MD simulation and molecular mechanic (MM) minimization were performed using GROMACS 4.5.3 package under Amber99 force fields (Van der Spoel *et al.*, 2005; Berendsen *et al.*, 1995; Hess *et al.*, 2008 and Lindahl *et al.*, 2001). Topologies of ligands were generated by acpype/Antechamber based on a General Amber Force Field (GAFF) (Sousa *et al.,* 2012). MD simulations were carried out in an NPT ensemble with periodic boundary conditions. Van der Waals forces were treated using a cut-off of 12 Å. The electrostatic interactions were calculated using the Particle-Mesh Ewald model with a 14 Å cut-off (Darden *et al.*, 1993).The complexes were solvated by a layer of water of at least 12 Å in all directions. The frequency to update the neighbor list was 10 ps. MD simulation was accomplished in four steps for each system. In the first step, the entire system was minimized using the steepest descent followed by conjugate gradient algorithms. In the second step, the solvent and Na^+ ions were allowed to evolve using minimization and molecular dynamics in the NVT ensemble for 500 ps and

in the NPT ensemble for 1000 ps at 100 K, where the initial configuration of the structures was kept fixed. In the third step, in order to obtain equilibrium geometry at 300 K and 1 atm, the system was heated at a weak temperature coupling ($\tau = 0.1$ ps) and pressure coupling ($\tau = 0.5$ ps). The Berendsenalgorithm was chosen for thermostat and barostat in equilibration phase (Berendsen *et al.*, 1984). To constrain the lengths of hydrogen-containing bonds, the LINCS algorithm was used (Hess *et al.*, 1997). The temperature of the system was then increased from 100 K to 300 K and the velocities at each step were re-accredited according to the Maxwell-Boltzmann distribution at that temperature and equilibrated for 200 ps. In the final (production) step, 20 ns MD simulations at 300 K with a time step of 2 fs was performed for each complex and final structures were obtained. The thermostat and barostat for production step were Nosé-Hoover thermostat and Parrinello-Rahmanbarostat (Berendsen *et al.*, 1984). In all simulations, two single strands of DNA were constrained to each other (Cheatham *et al*, 1998). Potential and kinetic energies and temperature at the last 5 ns were calculated using g_energy command of Gromacs package. Other analyses were performed by using Gromacs package.

3. MM/PBSA calculation

As indicated by Kumari, the binding free energy of a DNA molecule to a ligand molecule in a solution can be defined as:

$$\Delta G_{binding} = G_{complex} - (G_{DNA} + G_{ligand}) \qquad \text{Eq.1}$$

"A MD simulation is performed to generate a thermodynamically weighted ensemble of structures" (Kumari *et al.,* 2014). The free energy term is calculated as an average over the considered structures:

$$<G> = <E_{MM}> + <G_{solv}> - T<S_{MM}> \qquad \text{Eq.2}$$

Total molecular mechanical energies E_{MM} is calculated by using GROMACS utility with the AMBER99 force field. $-T<S_{MM}>$ is the solute entropic contribution. $G_{solvation}$ represents the free energy of solvation and consists of two parts: G_{polar} or G_{PB} and nonpolar contributions, $G_{nonpolar}$. G_{PB} is generated from the electrostatic potential between solute and solvents (Massova *et al.*, 1999).

In the current study, G_{polar} was calculated using the APBS (Adaptive Poisson-Boltzmann Solver program) method (Baker *et al.*, 2001) via the non-linearized Poisson Boltzmann equation. The non-polar contribution, $G_{nonpolar}$ was considered to be proportional to the solvent accessible surface area (SASA).

In the MM/PBSA approximation and for estimating $G_{free-DNA}$ and $G_{free-ligand}$, snapshots collected from the MD run for the DNA-ligand complex were used. After equilibration, snapshots of complex, DNA and ligand (without water molecules) were taken every 50 ps for calculating the enthalpy.

Binding free energy calculations based on the MM/PBSA approach can be performed either according to the three trajectories method (TTM) or according to the single trajectory method (STM). In our work, MM/PBSA calculations were performed according to the STM protocol. A single trajectory run for the complex is required for this method, whereby both the DNA and ligand structures are extracted directly from the complex structure (Huo *et al.*, 2002), thus zeroing out the E_{int} term. In this case, the DNA and the ligands are assumed to behave similarly in the bound and in the free forms.

In the MM/PBSA approximation, $E_{MM}+G_{solv}$ account for the enthalpy change is associated with complex formation. The computational determination of binding free energies requires the calculation of the entropic contributions to complex formation including conformational changes in the rotational, translational and vibrational degrees of freedom of the solute.

The MM/PBSA method was used by g_mmpbsa command (Baker *et al.*, 2001; Pronk *et al.*, 2013; Eisenhaber *et al.*, 1995 and Kumari *et al.*, 2014). In this module, entropic terms are not included and therefore it is unable to give the absolute binding energy. Thus, it is proper to calculate the relative binding energies for instance, to compare different ligands binds to the same receptor. In addition, the net entropic contribution is often small, and multiple studies have suggested that including corrections for changes in the configurational free energy of the system lead to only a small improvement in the total. We decided to neglect the entropic term in our calculations. The last 5 nanosecond of the MD simulations was considered for MM/PBSA calculations.

The energy components E_{MM}, G_{polar} and $G_{non-polar}$ of each complex were calculated for 100 snapshots extracted every 50 ps from the production trajectories at the last 5 ns. To calculate G_{polar}, a box was generated using the extremes coordinates of the molecular complex in each dimension. A coarse-grid box (cfac =3) was obtained when the box expanded in each dimension by two-fold. A finer grid-box is then placed within the coarse grid-box extending 50 Å (fadd=50) from the complex's extremes coordinates in each direction. An ionic strength of 0.6 M NaCl with radii of 0.95 and 1.81 Å, respectively for sodium and chloride ions was used during all G_{polar} calculations. The values for vacuum (vdie) and solvent (sdie) dielectric constants were taken as 1 and 80 respectively. The solute (pdie) dielectric constant was assigned a value of eight. Subsequently, the binding free energy of each snapshot was calculated for each complex using a combination of Eq.1 and 2 without entropic contributions in the binding energy (Kumari *et al.,* 2014 and Brown *et al.,* 2009 and Gohlke *et al.*, 2004 and Kar *et al.*, 2011

and Bradshaw *et al*., 2011).

Results and Discussion

1. Docking

Investigation of the docking results in Table 1 shows that the binding free energy of cladribine, fingolimod, modified cladribine (replacing OH on carbon 3′ ribose sugar with CH_3 group), the first and second modified fingolimod (removing one carbon or four carbons from the aliphatic hydrocarbon tail of fingolimod respectively) to

p53 sequence are negative; so these drugs are able to bind the *p53* promoter. Also, binding position of these ligands were mentioned. The positions of all compounds were in the minor groove of *p53* promoter. The binding position of cladribine and modified cladribine are 5′-T15T16G17-3′ nucleotide; and those of fingolimod,fm-fingolimod (first modified fingolimod) and sm-fingolimod (second modified fingolimod) to *p53* promoter are 5′-G30T31T32T33T34-3′ nucleotides.

Table 1. Van der Waals (VDW)contribution, Electrostatic contribution (Elec) and the lowest binding free energy (L.B) of native and modified cladribine, fingolimod to p53 promoter, nucleotides15-34 are shown.

Compound	VDW + Hbond + desolvation Energy(kcal/mol)	Elec (kcal/mol)	L.B (kcal/mol)	Sequence of binding position
Cladribine	-5.32	-0.1	-3.93	5′- T15T16G17-3′
Modified cladribine	-5.5	-0.07	-5.47	5′-T15T16G17-3′
Fingolimod	-8.99	-1.72	-7.69	5′-G30T31T32T33T34-3′
Fm-Fingolimod[1]	-7.75	-1.90	-7.21	5′-G30T31T32T33T34-3′
Sm-fingolimod[2]	-6.88	-1.91	-7.03	5′-G30T31T32T33T34-3′

1. First modification of fingolimod (i.e. deleting one carbon of fingolimod tail).
2. Second modification of fingolimod (i.e. deleting four carbon of fingolimod tail).

These sequences are the positions of binding of transcription factors such as USF (upstream stimulatory factor) or TFE3 (transcription factor E3) (Kim *et al.*, 2008; Yasumoto *et al.*, 1994). Binding free energy of modified cladribine to *p53* promoter is lower than that for cladribine, it means that the binding of modified cladribine is stronger than that for cladribine but binding free energy of the first and second modified fingolimod to *p53* promoter are more than that for fingolimod, it means that the first and the second modified

fingolimod are weaker to bind *p53* promoter. In all cases, Van der Waals (plus Hbond and desolvation) contributions are more negative and more important than electrostatics interactions (Table 1).

2. Molecular dynamics simulation

Table 2 shows the results of average potential and kinetic energies, temperature, root mean square deviation (RMSD) of *p53* promoter and ligands RMSD relative to initial positions during the last 5 ns of 20 ns MD simulation.

There are small variations in potential and kinetic energy, temperature and RMSD of the *p53* promoter during the last 5 ns of MD simulation with a very low ratio of the total energy drift to the average total energy (Table 3). This shows that the simulations were sufficient and stable under the simulation conditions and thermal equilibrium of the systems. By investigating the final structures of 20 ns MD simulation it appeared that the two strands of the *p53* promoter remained together during 20 ns simulations.

Table 2. The potential energy (P), kinetic energy (K) and temperature (T) and radius of gyration (Rg) and RMSD of *p53* promoter and drugs at complex during the last 5 ns of MD simulations.

Name	P (kcal/mol)	K (kcal/mol)	T (K)	RMSD of Drug at complex (nm)*	RMSD of p53 Promoter at Complex (nm)	Rg of p53 promoter at complex (nm)
Cladribine	-128200(170)	20116.3(210)	299.9(3.1)	0.07(0.02)	0.74(0.08)	4.87(0.05)
Modified cladribine	-127480(185)	20009(212)	300.1(3.2)	0.16(0.02)	1.24(0.72)	5.04(0.18)
Fingolimod	-126822(172)	19944(206)	299.75(3)	0.19(0.05)	0.78(0.1)	4.87(0.09)
Fm-Fingolimod[1]	-127028(173)	19996(218)	300(3.27)	0.2 (0.03)	0.9 (0.11)	4.89(0.06)
Sm-fingolimod[2]	-126637(173)	19932(216)	300.1(3.2)	0.16(0.03)	0.9 (0.32)	4.91(0.11)

1. Fm-Fingolimod:First modification of fingolimod (i.e. deleting one carbon of fingolimod tail);
2. Sm-Fingolimod: Second modification of fingolimod (i.e. deleting four carbon of fingolimod tail).
*. Nanometer

Table 3: The ratio of the total energy drift to average of total energy during 20 ns MD simulations of all species.

System name	Ratio of the total energy drift to average of total energy ($\times 10^{-5}$)
Cladribine	4.38
Modified cladribine	5.52
Fingolimod	2.27
Fm-fingolimod[1]	5.07
Sm-fingolimod[2]	7

1. Fm-Fingolimod: First modification of fingolimod (i.e. deleting one carbon of fingolimod tail)
2. Sm-Fingolimod: Second modification of fingolimod (i.e. deleting four carbon of fingolimod tail).

Also, small RMSDs of ligand atoms during simulation relative to the starting position (Table 2) showed that the ligands reach to stable positions.

To determine the relative populations of all conformations, the trajectories were clustered using g_cluster command of the Gromacs package. Two conformations were considered neighbors if the backbone RMSD between them was less than 0.2 nm.

The middle structure of the most populated structures obtained from clustering of trajectories during the last 5 ns of MD simulation showed that cladribine and modified cladribine stay in the minor groove of *p53* promoter in 5´-T16G17A18-3´ sequence however, fingolimod,

the first and second modified fingolimod go

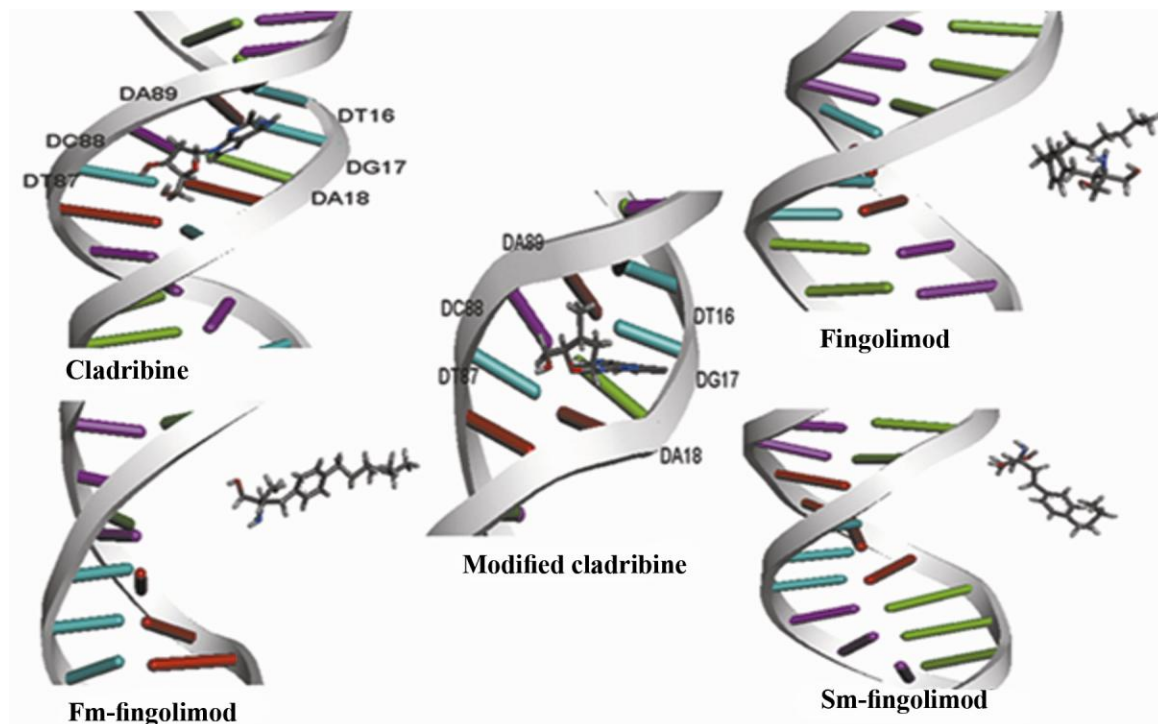away from their initial docking positions (Fig. 2).

Figure2. The middle structure of the most populated structures of drugs-DNA complex during the last 5 ns MD simulation.The number of the nucleotides in double strandedp53 promoter was mentioned in Table 4. fm-fingolimod: First modification of fingolimod,i.e. deleting one carbon of fingolimod tail. sm-fingolimod: Second modification of fingolimod, i.e. deleting four carbon of fingolimod tail.

The number of nucleotides in double-stranded *p53* promoter has been indicated in Table 4. In the middle structure of the most populated structures of cladribine (belongs to 19.6 ns) and modified cladribine (belongs to 18.68 ns) in complex with *p53* promoter, guanosine 17 (H22 and N3 and O4′ atoms) and adenosine 89 (N3 atom) of double stranded *p53* promoter, have hydrogen bonds with cladribine. In middle structure of the most populated structures of MD simulation of fingolimod (belongs to 17.94 ns), first modified

fingolimod (belongs to 17.1 ns) and second modified fingolimod (belongs to 16.98 ns), no hydrogen bonds seen with *p53* promoter.

The average solvent accessible surface area (SASA) of the ligand atoms during the 20 ns MD simulation were calculated by g_sas command and non-hydrogen atoms with SASA less than 10 Å^2 were determined. These atoms probably bind to the *p53* promoter during MD simulation. The results showed that cladribine bind the *p53* promoter via its N2, N4, O1, C3, C2 and N3 atoms (these atoms were shown in Fig. 1A).

Table 4. The frequency of nucleotides in double-stranded p53 promoter.

Nucleotide Number	DNA strand direction:5´	DNA strand direction: 3´	Nucleotide Number
1	G	C	104
2	A	T	103
3	G	C	102
4	C	G	101
5	C	G	100
6	T	A	99
7	C	G	98
8	G	C	97
9	C	G	96
10	A	T	95
11	G	C	94
12	G	C	93
13	G	C	92
14	G	C	91
15	T	A	90
16	T	A	89
17	G	C	88
18	A	T	87
19	T	A	86
20	G	C	85
21	G	C	84
22	G	C	83
23	A	T	82
24	T	A	81
25	T	A	80
26	G	C	79
27	G	C	78
28	G	C	77
29	G	C	76
30	T	A	75
31	T	A	74
32	T	A	73
33	T	A	72
34	C	G	71
35	C	G	70
36	C	G	69
37	C	G	68
38	T	A	67
39	C	G	66
40	C	G	65
41	C	G	64
42	A	T	63
43	T	A	62
44	G	C	61
45	T	A	60
46	G	C	59
47	C	G	58
48	T	A	57
49	C	G	56
50	A	T	55
51	A	T	54
52	G	C	53
	DNA strand direction: 3´	DNA strand direction: 5´	

Modified cladribine bind the *p53* promoter via its N2, N4, O1, C3, C7, C2, N3 and C8 atoms (Fig. 1A). In fingolimod and first modification only, three atoms (i.e. C16, C1 and C4) and in second modified fingolimod only, three atoms (i.e. C13, C5 and C8) (Fig. 1B) have SASA less than 10 Å^2.

Table 5 shows the average number of hydrogen bonds between ligands and the *p53* promoter.

Minimum distance between *p53* promoter and ligands and the number of contacts less than 0.6 nm between *p53* promoter and ligands during the last five ns of MD simulations were also mentioned in Table 5. Figure 3 shows minimum distance between *p53* promoter and ligands and the number of contacts less than 0.6 nm between *p53* promoter and ligands during the 20 ns MD simulation.

Table 5. The average number of hydrogen bonds between ligands and p53 promoterand minimum distance between them and number of contacts <0.6 nm between them during the last 5 ns of MD simulations

Complex	Average number of hydrogen bonds between DNA and drug	Minimum distance between DNA and drug (nm)	Number of contacts <0.6 nm between DNA and drug
Cladribine	2(0.97)	0.19(0.013)	31(0.1)
Modified cladribie	2.53(0.73)	0.19(0.01)	32.22(1.21)
Fingolimod	0.14(0.43)	0.62(0.3)	5.4(7.6)
Fm-Fingolimod[1]	0.06(0.31)	0.65(0.26)	5.31(9.66)
Sm-fingolimod[2]	0.25(0.6)	0.58(0.31)	7.36(8.94)

1. Fm-Fingolimod: First modification of fingolimod (i.e. deleting one carbon of fingolimod tail);
2. Sm-Fingolimod: Second modification of fingolimod (i.e. deleting four carbon of fingolimod tail).

The maximum number of hydrogen bonds present in *p53* promoter belongs to cladribine and modified cladribine, and this parameter is similar in them. Then their interactions with *p53* promoter are strong (Table 5). In addition, the number of hydrogen bonds between fingolimod, first or second modified fingolimod are the same but lower than those between cladribine and modified cladribine. This means that the interaction of fingolimod and its derivates with *p53* promoter is weak.

These results were confirmed by the minimum distance between ligands and *p53* promoter and also the number of contacts between them (Fig. 3). In addition, first modified fingolimod (fm-fingolomod) has the most minimum distance and the least number of contacts with *p53* promoter among fingolimod and its derivatives. However, these parameters are more proper in second modification of fingolimod (sm-fingolomod) and its interaction with *p53* promoter is stronger relative to native or first modified fingolimod (Table 5).
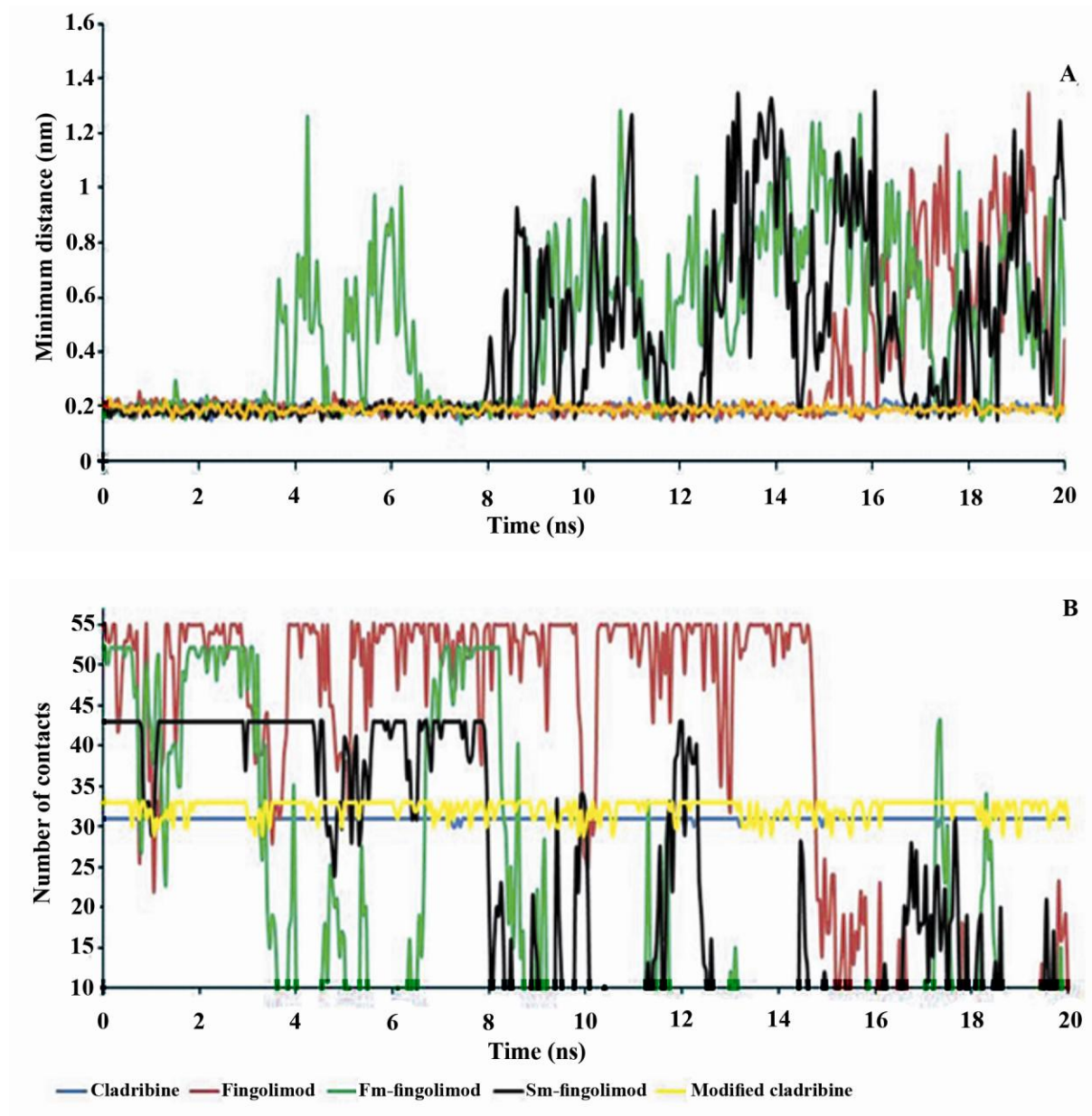
Figure 3. The minimum distance (A) and the number of contacts less than 0.6 nm between p53 promoter and drugs (B) during 20 ns of MD simulations. Fm-fingolimod: First modification of fingolimod,i.e. deleting one carbon of fingolimod tail. Sm-fingolimod: Second modification of fingolimod, i.e. deleting four carbon of fingolimod tail.

3. Binding free energy results

Table 6 shows binding free energy (ΔG_b), Van der Waals and electrostatic energies of all ligands with *p53* promoter obtained from 100 snapshots during the last 5 ns of MD simulation. Binding free energy of cladribine, modified cladribine and second modified fingolimod to the *p53* promoter is negative.

This means that these drugs can bind the *p53* promoter and through inhibition of the *p53* gene transcription probably induce cancer; then they can be supposedly carcinogen.

Nevertheless, binding free energy of fingolimod and first modified fingolimod to *p53* promoter is positive, so they may not bind the *p53* promoter.

Table 6. MM/PBSA binding free energies (kcal/mol) for ligand/DNA complexes during the last 5 ns of MD simulation

Complex name	ΔE_{elec}	ΔE_{vdw}	ΔG_{polar}	$\Delta G_{non\text{-}polar}$	$\Delta G_{binding}$
Cladribine	-22.92(1.72)	-29.38(0.72)	10.21(0.43)	-0.43(0.06)	-42.68(1.94)
Modified Cladribine	-14.38(1.35)	-20.77(0.66)	14.25(0.70)	-0.05(0.05)	-20.86(1.65)
Fingolimod	-1.43(1.44)	-0.78(0.20)	2.83(2.12)	1.68(0.23)	2.19(2.45)
Fm-Fingolimod[1]	-2.16(1.67)	-1.08(0.32)	6.01(2.16)	1.09(0.23)	3.98(3.04)
Sm-fingolimod[2]	-7.64(2.09)	-1.32(0.33)	6.54(2.65)	0.65(0.22)	-1.73(2.74)

1. Fm-Fingolimod: First modification of fingolimod (i.e. deleting one carbon of fingolimod tail);
2. Sm-Fingolimod: Second modification of fingolimod (i.e. deleting four carbon of fingolimod tail).
Abbreviations: ΔE_{elec} = Electrostatic energy of interaction, ΔE_{vdw} = Van der Waals energy of interaction. ΔG_{polar}=polar solvation free energy, $\Delta G_{non\text{-}polar}$= Non-polar solvation free energy.

Binding free energy of modified cladribine to the *p53* promoter is more positive and weaker than native cladribine. The results obtained from binding free energy (Table 6) and docking (Table 1) for modified cladribine are opposite. Of course, results obtained from MD simulation are more accurate than those from dockings since water molecules and ions explicitly present in molecular dynamics simulation and MM/PBSA calculations, but in dockings implicit solvent utilized and therefore water molecules and ions do not exist. This suggests that MD simulation and MM/PBSA calculations are more accurate, and modified cladribine than to cladribine has a weaker interaction with *p53* promoter.

The negative binding free energy of the dockings and MM/PBSA method are consistent with visual inspection of the middle structures of the most populated structures obtained from MD simulation (Fig. 2).

MM/PBSA results show that binding of cladribine to the *p53* promoter is more negative than fingolimod which means that cladribine probably is a powerful inhibitor in initiation of *p53* gene transcription. This may be due to the similarity of purine rings of cladribine to adenosine. The results of MM/PBSA calculations shows that as compare with the native fingolimod, if one carbon is taken from fingolimod (Fm-Fingolimod), binding free energy (ΔG_b) increases but it decreases when four carbons (sm-fingolimod) are removed (Table 6). These results are consistent with MD simulation (Table 5 and Fig. 3) but contrasted with docking results

(Table1). Reducing four carbons from the aliphatic tails of fingolimod increases binding strength of fingolimod to the *p53* promoter. Then it is an inappropriate modification for fingolimod and it can be investigated through empirical studies. There is a very good coordination between the average number of hydrogen bonds during simulation and binding free energy (Tables 5, 6). Also the differences in the Van der Waals free and bound energies of all drugs during the last 5 ns MD simulation were calculated. According to the MM/PBSA results, the Van der Waals interactions are more important (more negative) and more favorable for interactions of cladribine and modified cladribine with *p53* promoter. Electrostatic interactions are more important

and more favorable for interactions of fingolimod and its derivatives with *p53* promoter (Table 6). This suggests that the mechanism underlying interactions of cladribine and fingolimod with *p53* promoter are different.

The number of the first ten nucleotides with the most total energy contributions in binding of ligands to the *p53* promoter were mentioned in Table 7. As seen 3´-A89C88A90T87-5´ or 5´-T16G17A18T19G20G21-3´ sequence has a favorable interaction with cladribine however, 5´-G17A18T19G20G21-3´ sequence has a favorable interaction with modified cladribine (Tables 6 and 7). Interactions of fingolimod and its derivatives are weak and interaction energies are below -1.1 kcal/mol (Table 7).

Table 7.The first ten nucleotides that have the most total energy contribution in binding of drugs to p53 promoter (number of nucleotides are as mentioned in Table 4)

	Cladribine			Modified cladribine			Fingolimod			Fm-Fingolimod[1]			Sm-fingolimod[2]		
Num	Nuc	TE	Num	Nuc	TE	Num	Nuc	TE	Num	Nuc	TE	Num	Nuc	TE
89	A	-27.04(1.15)	17	G	-24.42(0.89)	22	G	-1.03(0.46)	72	A	-0.50(0.19)	76	C	-1.11(0.64)
88	C	-16.56(1.11)	18	A	-9.87(0.66)	21	G	-0.52(0.35)	74	A	-0.46(0.35)	29	G	-1(0.75)
18	A	-15.31(0.82)	19	T	-7.80(0.77)	68	G	-0.44(0.25)	77	C	-0.38(0.49)	82	T	-0.8(0.84)
90	A	-13.49(1.21)	89	A	-7.26(1.13)	23	A	-0.44(0.31)	73	A	-0.38(0.25)	18	A	-0.58(0.28)
19	T	-10.83(0.82)	90	A	-4.00(0.67)	94	C	-0.42(0.16)	71	G	-0.34(0.25)	77	C	-0.57(0.42)
87	T	-6.55(0.71)	20	G	-2.47(0.49)	59	C	-0.33(0.18)	1	G	-0.24(0.17)	30	T	-0.56(0.3)
20	G	-3.81(0.36)	88	C	-2.20(0.45)	66	G	-0.31(0.17)	24	T	-0.23(0.3)	31	T	-0.49(0.18)
86	A	-2.96(0.25)	87	T	-1.11(0.25)	88	C	-0.31(0.20)	35	C	-0.21(0.23)	69	G	-0.44(0.33)
16	T	-2.07(0.69)	21	G	-0.78(0.18)	2	A	-0.29(0.22)	31	T	-0.18(0.28)	32	T	-0.43(0.16)
21	G	-1.85(0.23)	86	A	-0.46(0.13)	46	G	-0.29(0.16)	51	A	-0.15(0.17)	28	G	-0.36(0.38)

Notes:
1.Fm-Fingolimod: First modification of fingolimod (i.e. deleting one carbon of fingolimod tail).
2. Sm-Fingolimod: Second modification of fingolimod (i.e. deleting four carbon of fingolimod tail).
Num= Number of nucleotide in p53 promoter, Nuc=Nucleotide name, TE=Total energy of interaction each nucleotide with p53 promoter.

Conclusions

In this in silico study we showed a difference

in the binding of cladribine and fingolimod and some of their derivatives to the *p53* promoter.

This finding was confirmed by docking, molecular dynamics simulation and MM/PBSA methods.

Based on the in silico studies it has been demonstrated that both cladribine and modified cladribine (replacing -OH on carbon 3′ ribose sugar of adenosine with -CH$_3$) can bind the minor groove of *p53* promoter and may lead to conformational changes in*p53* promoter. These drugs can cause qualitative changes in the *p53* gene and modulate the p53-mediated carcinogenesis. MD simulation and MM/PBSA calculations showed that by modification of cladribine its interactions decreases and the modified cladribine may be less carcinogenic than cladribine, assuming that the former compound is a more favorable modification. This phenomenon is explained by knowing the increased cladribine size and steric prohibition with minor grove of *p53* promoter. In addition, an energetic analysis revealed that hydrophobic interactions relative to electrostatics interactions are more important for binding of cladribine to *p53* promoter. Removal of one carbon atom from the aliphatic tails of fingolimod increased the binding free energy whereas binding free energy decreased by deletion of four carbon atoms. It is suggested that modifications in fingolimod or cladribine structure may provide an interesting new direction for drug development. In the future studies, it is suggested to investigate the effect of 2-chloro-2′-deoxy adenosine triphosphate (CldATP) (Foley *et al.*, 2004) and fingolimod phosphate (Cohen *et al.*, 2007) on *p53* gene promoter since they are produced by some enzymes in the cell. Moreover, the effect of these drugs on exons of *p53* gene is worth studying.

Acknowledgment

References

[1] Berendsen HJC, Postma JPM, Van Gunsteren WF, Dinola A, Haak JR. 1984. Molecular dynamics with coupling to an external bath. J ChemPhys 81:3684-3690.

[2] BaiL, Zhu WG. 2006. p53: structure, function and therapeutic applications. J Cancer Mol 2(4):141-153.

[3] Berendsen HJC, Van der Spoel D, Van Drunen R. 1995. GROMACS: A message - passing parallel molecular dynamics implementation. Computer Physics Communications 91:43-56.

[4] Baker NA, Sept D, Joseph S, Holst MJ, McCammon JA. 2001. Electrostatics of nanosystems: Application to microtubules and the ribosome. ProcNatlAcadSci

98(18): 10037-10041.

[5] Brown SP, Muchmore SW. 2009. Large-scale application of high-throughput molecular mechanics with poisson-Boltzmann surface area for routine physics-based scoring of protein-ligand complexes. J Med Chem 52(10):3159-3165.

[6] Bradshaw RT, Patel BH, Tate EW, Leatherbarrow RJ, Gould IR. 2011. Comparing experimental and computational alanine scanning techniques forprobing a prototypical protein-protein interaction. Protein Eng Des Sel 24(1–2): 197-207.

[7] Calabresi P. 2004. Diagnosis and management of multiple sclerosis. American family physician 70:1935.

[8] Cheatham TE, Srinivasan J, Case DA, Kollman PA. 1998. Molecular dynamics and continuum solvent studies of the stability of polyG-polyC and polyA-polyT DNA duplexes in solution. J Biomol Struct Dyn 16(2):265-280.

[9] Cohen B, Rieckmann P. 2007. Emerging oral therapies for multiple sclerosis. International journal of clinical practice 61:1922-1930.

[10] Darden T, York D, Pedersen L. 1993. Particle meshEwald - An N.log (N) method for Ewald sums in large systems. J ChemPhys98:10089-10092.

[11] Elizondo-Riojas MA, Kozelka J. 2001. Unrestrained 5 ns molecular dynamics simulation of a cisplatin-DNA 1, 2-GG adduct provides a rationale for the NMR features and reveals increased conformational flexibility at the platinum binding site. Journal of molecular biology 314:1227-1243.

[12] Eisenhaber F, Lijnzaad P, Argos P, Sander C, Scharf M. 1995. The Double Cube Lattice Method: Efficient Approaches to Numerical Integration of Surface Area and Volume and to Dot Surface Contouring of Molecular Assemblies J Comp Chem 16(3):273-284.

[13] Francesca B. 2007. Application of Interferon Beta-1b in Multiple Sclerosis 19:22-30.

[14] Foley TT, Hentosh P, Walters DE. 2004. 2-Chloro-2'-deoxyadenosine: alteration of DNA: TATA element binding protein (TBP) interactions. Journal of molecular modeling 10:32-37

[15] Frisch, M.J. et al., .1998. Gaussian 98 (Gaussian, Inc., Pittsburgh, PA).

[16] Gohlke H, Case DA. 2004. Converging free energy estimates: MM-PB(GB)SA studies on the protein-protein complex ras-raf. J ComputChem 25(2):238-250.

[17] Hess B, Bekker H, Berendsen HJC, Fraaije JGEM. 1997. LINCS: a linear constraint solver for molecular simulations. J Comp Chem18:1463-1472.

[18] Hess B, Kutzner D, Lindahl E. 2008. Gromacs 4: Algorithms for highly efficient, load-balanced, and scalable molecular simulation. J Chem Theory Comput 4:435-447.

[19] Huo S, Massova I, Kollman PA. 2002. Computational alanine scanning of the 1:1 human growth hormone-receptor complex. J ComputChem 23(1):15-27.

[20] Kar P, Lipowsky R, Knecht V. 2011. Importance of polar solvation for cross-reactivity of antibody and its variants with steroids. J PhysChem B 115:7661-7669.

[21] Kumari R, Kumar R, Consortium OSDD, Lynn AM. 2014. g_mmpbsa-A GROMACS Tool for High-Throughput MM-PBSA Calculations. J ChemInf Model Article ASAP.

[22] Karplus M, Kuriyan J. 2005. Molecular dynamics and protein function. ProcNatlAcadSci 102(19):6679–6685.

[23] Kim JS, Jamil M, Jung JE, Jang JE, Lee JW, Ahmad F, Woo MK, Kwak JY, Jeon YJ. 2011. Rotational viscosity calculation method for liquid crystal mixture using molecular dynamics 12(3):135-139.

[24] Kim KS, Jung HS, Chung YJ, Jung TS, Jang HW, Lee MS, Kim KW, Chung JH. 2008. Overexpression of USF increases TGF-beta1 protein levels, but G1 phase arrest was not induced in FRTL-5 cells. J Korean Med Sci 23(5):870-876.

[25] Lindahl E, Hess B, Van der Spoel D. 2001. GROMACS 3.0: a package for molecular simulation and trajectory analysis. Journal of Molecular Modeling 7:306-317.

[26] Morris G, Goodsell D, Halliday R, Huey R, Hart W, Belew R, Olson A. 1998. Automated docking using a Lamarckian genetic algorithm and an empirical binding free energy function. Journal of computational chemistry 19(14):1639-1662.

[27] Massova I, Kollman PA. 1999. Computational alanine scanning to probe protein-protein interactions: A novel approach to evaluate binding free energies. JACS 121(36):8133-8143.

[28] Majumdar R, Railkar R, Dighe RR. 2011. Docking and free energy simulations to predict conformational domains involved in hCG-LH receptor interactions using recombinant antibodies. Proteins: Structure, Function, and Bioinformatics 79(11):3108-3122.

[29] Navikas V, Link H. 1996. Review: cytokines and the pathogenesis of multiple sclerosis. Journal of neuroscience research 45:322-333.

[30] Neidle S, Pearl LH, Skelly JV. 1987. DNA structure and perturbation by drug binding. Biochemical Journal 243(1):1-13.

[31] Oostenbrink C, Gunsteren WFV. 2005. Free energies of ligand binding for structurally diverse compounds. Proc Natl

Acad Sci 102:6750-6754.

[32] Pronk S, Pãll S, Schulz R, Larsson P, Bjelkmar P, Apostolov R, et. al. 2013. GROMACS 4.5: a high-throughput and highly parallel open source molecular simulation toolkit. Bioinformatics 29 (7): 845-854.

[33] Reisman D, Rotter V. 1993. The helix-loop-helix containing transcription factor USF binds to and transactivates the promoter of the *p53* tumor suppressor gene. Nucleic acids research 21(2):345-350.